

Computational Investigation of Icing Conditions on The Velocity Profiles of a Commercial Aircraft

T. Satheesh^a and J. Bruce Ralphin Rose^b

Dept. of Aeronautical Engg., Regional Campus, Anna University, Tirunelveli, India

^aCorresponding Author, Email: tsatheesh4u@gmail.com

^bEmail: bruce@autvtl.ac.in

ABSTRACT:

Icing is a challenging problem in the aerospace environment especially for inter-continental airline operations. Existing anti-icing methods offer consistent performance against glaze icing problems however it compromises the fuel efficiency through by-pass bleed air. A Numerical analysis for an airfoil with and without icing conditions is done to investigate the velocity distribution around the commercial airplane wing. The supercritical airfoil is analyzed in step by step ice accretion aspect under optimal velocity input about 175 m/s. The surrounding temperature is maintained in the range of 273K to 243K as per FAR standards at various angles of attack. The airfoil is designed by DESIGN MODELER module exists in ANSYS workbench and it is meshed with ICEMCFD. Subsequently, it is analyzed with the help of a flow solver at various time steps of ice accretion to verify the dynamic pressure changes due to rime icing. The iced airfoil produced realistic CL and CD variations for different ice shapes against the clean wing configuration. The step by step ice accretion is summarized and the roadmap for ice elimination through coating techniques is proposed.

KEYWORDS:

Icing problem; Velocity distribution; Fluent; Wind tunnel testing

CITATION:

T. Satheesh and J.B.R. Rose. 2016. Computational investigation of icing conditions on the velocity profiles of a commercial aircraft, *Int. J. Vehicle Structures & Systems*, 8(4), 219-223. doi:10.4273/ijvss.8.4.07.

ACRONYMS AND NOMENCLATURE:

2D	Two-dimensional
3D	Three-dimensional
AOA	Angle of attack
CFD	Computational fluid dynamics
C_p	Pressure coefficient
C_l	Lift coefficient
LE	Leading edge
TE	Trailing edge
LWC	Liquid water content
V	Velocity

1. Introduction

Ice accretion occurs on the airplane surfaces as the air temperature is 0°C or less in the presence of moisture content [1]. The most significant hazard of icing is the perturbation of airflow over aircraft surfaces. This perturbation in airflow reduces lift and increases drag, causing the airplane to stall at a lower Angle of Attack (AoA). Static ice has unusual inherent structural shapes and properties from impact Liquid Droplet Contents (LWC) [2]. Ice accretion takes place also in the engine intake, blocking the airflow to the engine that causes engine failure. Many light airplanes are not authorized to fly into known icing conditions according to the Federal Aviation Requirements (FAR) norms. Larger aircrafts are equipped with anti-icing systems or conventionally de-icing systems [3]. The presence of even a very thin layer of ice can limit the functions of wings, propellers,

windshields, antennas, vents, intakes and cowlings. For example, ice accumulated on the horizontal tail stabilizer reduces its ability to achieve the trim condition and causes tail stall.

Because of all these problems significant effort has been taken to develop surfaces that slow down ice formation at various altitudes. Most of these efforts involve chemical, thermal and mechanical techniques for removing ice that has already accumulated [4]. It is well known that the bleed air from the airplane power plant heats the inlet cowls and prevent ice formation. Bleed air can also be ducted to wings to heat the wings in the vicinity of the leading edge. Heaters are used to prevent ice formation on pitot tubes, stall vanes and temperature probes. Electrical heat provides anti-icing for external airplane instruments such as propellers, windshields and pitot tubes. In the same fashion, wind energy sector also faces ice accretion on the turbine blades of the wind mill [5]. The recent research strategies are showing great improvement for creating ice phobic surfaces. Knowledge of the contact line shape and of the contact angle distribution along the contact line is fundamental to estimate the adhesion force of a liquid drop [6]. Although currently available systems for ice removal are effective, it requires continuous supply of hot air or chemicals or electric power.

A coating on the aerodynamic surface enhances the effectiveness of de-icing system but the life of the coated material and its water repelling abilities are not yet established [7]. Superhydrophobic coatings are water

repellent surfaces [8-9], on which liquid water adhesion is found to be low under standard conditions. However, defining the contact angle is critical as the angle a sessile drop forms when placed on a surface and the term superhydrophobic is usually mentioned to surfaces with high contact angles ($>150^\circ$) [10] with low contact angle hysteresis [11]. The structure of the surface thus increases the water-repellence [12] significantly, and water drops formed on it readily roll off [13]. The scheme of using superhydrophobic coatings is to take the benefit of water-repellence and low adhesion of drops in liquid state to such coatings to reduce or eliminate water accumulation on the surface before it freezes. The icing affects the entire Lift Coefficient (CL) and Drag Coefficient (CD) of the airplane as displayed in Fig. 1.

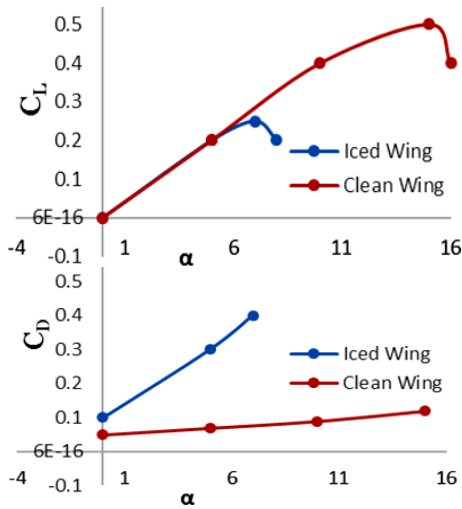


Fig. 1: CL vs. AoA (Top) and CD vs. AoA (Bottom) plots

Modelling of the icing conditions experimentally determines:

- The mass rate of water impingement on the airfoil (water intercepted)
- The area of impingement
- The distribution of the water over this area.

The mass rate of impinging water gives the indication of the quantity of the water that must be maintained at a liquid state until it either evaporates or runs off the trailing edge. It helps to avoid the formation of ice after the area of impingement, normally termed as runback. Hence, the experimental procedure is very difficult to achieve and the required conditions exist in the laboratory are expensive. Alternatively, the computational investigation is preferred for icing investigation and the results are compared with a NASA research article [14].

2. Computational investigation

Computation of the airflow over an ice accreted commercial airplane wing is done with ANSYS Fluent solver. Its Reynolds Average Navier-Stokes (RANS) flow equation model is selected for the present problem with a supercritical airfoil configuration (NACA XX-X18).

2.1. Grid generation

ANSYS ICEM CFD was utilized to mesh the airfoil model and control volume. The control volume is

created on the boundary of around 14C to clearly study about the far field variations. Unstructured triangular meshes are used and the region around the airfoil surface is fine meshed to acquire precise results. The mesh consists of 3,03,692 nodes and 3,03,468 elements with the minimum sizing of 3.8574 mm and the growth rate is set to 1.2. Fig. 2 shows the meshed airfoil that is fully covered with ice bubbles accretion on the upper surface. The mesh smoothing process is done near the solid boundary to speed up the solution convergence in the fluent solver.

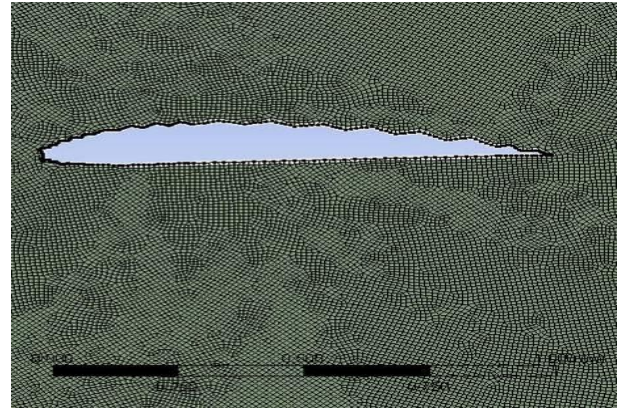


Fig. 2: Meshed airfoil with ice on the top surface

2.2. CFD solver

FLUENT is a commercial CFD package that is utilized to solve the compressible RANS equations on the grids created for the iced airfoil model inside the control volume. The 2D FLUENT analysis is performed using pressure based conditions with energy equation in the Spalart-Allmaras (SA1-equation) coupled scheme. Solution method for pressure is standard whereas for density and moment it is chosen as second order upwind. The control volume is set to 14 times of chord and the other boundary conditions are listed in Table 1.

Table 1: Boundary condition

Boundary	Parameters
Inlet	Velocity inlet
Outlet	Pressure outlet
Far field	Pressure far field
Wall	Stationary wall
Velocity	175 m/s
Temperature	243 K
AoA	0°, 3°, 6°

2.3. CFD Results and discussion

The iced airfoil is analyzed based on the step by step ice accretion process under similar conditions at different AoA. Fig. 3 shows the reference dynamic pressure profile at 0° AoA without any ice formation on the airfoil surface. Max dynamic pressure obtained at 0° AoA is 31.2 kPa. The appropriate velocity magnitudes can be obtained from the dynamic pressure profiles by $q = 0.5\rho V_\infty^2$. Here, ρ is the density to be assumed according to the cruising altitude of the airplanes. The maximum dynamic pressure occurs at the top of the airfoil and hence satisfying the real condition. The obtained value is noted and referred for further analysis.

The dynamic pressure increases to 33.4kPa from 31.2kPa as the AoA increases and the values are obtained to compare with the iced profiles is shown in Fig. 4. The dynamic pressure increases from 33.4kPa to 36.2kPa as the angle of attack increases when compared with the above result shown in Fig. 5. It shows that the dynamic pressure increases on the upper surface as the AoA increases and leading to the large increment in C_L .

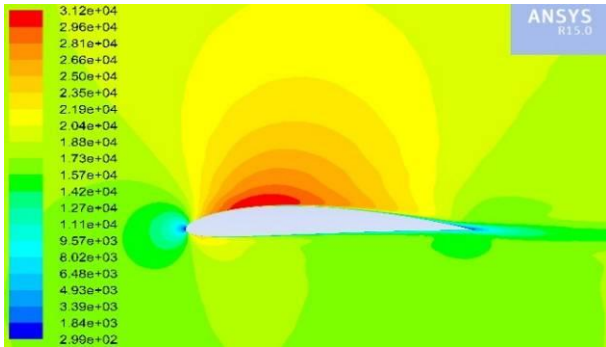


Fig. 3: Dynamic pressure profile without ice (0° AoA)

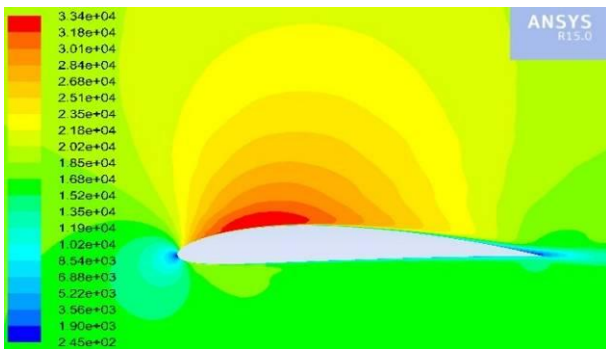


Fig. 4: Dynamic pressure profile without ice (3° AoA)

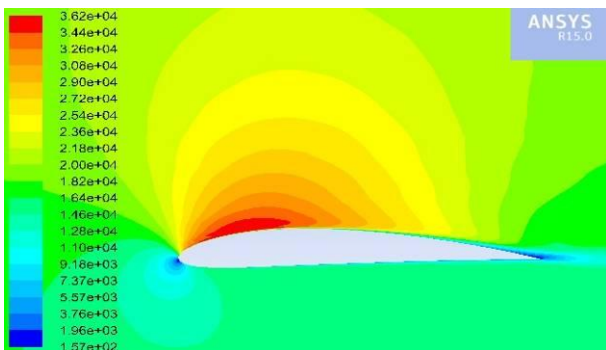


Fig. 5: Dynamic pressure profile without ice (6° AoA)

Fig. 6 shows the dynamic pressure profile at 0° AoA with the leading edge ice accretion. The dynamic pressure increases to 37kPa from 31.2kPa as the ice starts to grow on the leading edge of the airfoil. Thus it affects the dynamic pressure profile significantly as compared with the no ice conditions highlighted in Fig. 3. The velocity distribution starts to increase when the ice bubbles/droplets begin to accumulate on the airfoil. The leading edge has the dynamic pressure of about 5.5kPa due to the ice formation on the leading edge and the maximum dynamic pressure of 37kPa occurs at the top surface of the airfoil. In Fig. 7, dynamic pressure is increased to 38.2kPa from 33.4kPa, thus affecting the dynamic pressure profile though the AoA is increased slightly. It is an obvious fact that it occurs because of the

accretion of ice on the leading edge of the airfoil. When compared with the no icing condition, the dynamic pressure has been decreased at the same AoA with same initial dynamic pressure. The dynamic pressure at the leading edge is around 9.7kPa and it is due to the ice formation and the maximum dynamic pressure occurs at the top surface around 38.2kPa.

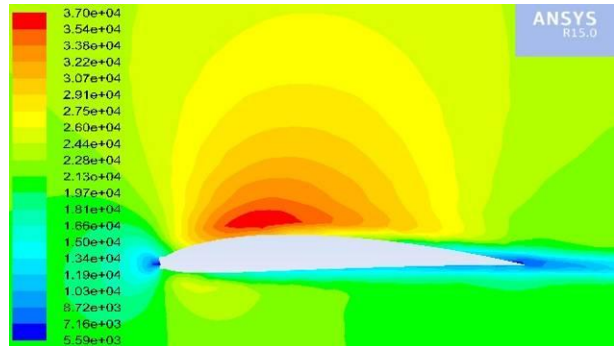


Fig. 6: Dynamic pressure profile L.E ice (At 0° AoA)

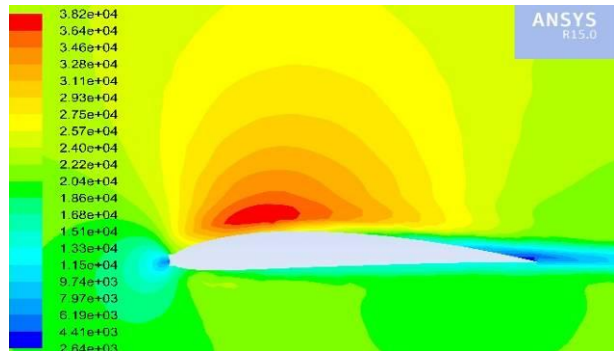


Fig. 7: Dynamic pressure profile L.E ice (At 3° AoA)

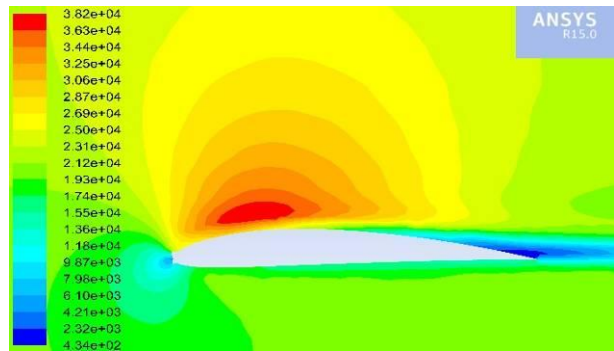


Fig. 8: Dynamic pressure profile L.E ice (At 6° AoA)

Fig. 8 shows the dynamic pressure profile at 6° AoA with leading edge rime ice accretion. The dynamic pressure change is clearly observed in this AoA from 36.2kPa to 38.2kPa at the initial stage of ice formation and the contour is briefly studied. It shows the upturn in dynamic pressure because of the formation of ice at the leading edge. This explains how the aerodynamic forces and boundary layer flow separation characteristics are affected due to ice accretion problem [15]. Since, it is just the starting point of small scale ice formation the results for higher ice accretion are analyzed and summarized. The dynamic pressure at leading edge is around 9kPa due to the ice formation and the maximum dynamic pressure of 38.2kPa occurs at the upper surface of the airfoil (Exactly at the Aerodynamic Centre).

Fig. 9 presents about the dynamic pressure profile at 0° AoA with complete ice accretion at the top surface. However, the intermediate small scale icing profiles have been investigated and their influence on the pressure coefficient (C_p) is studied. Fig. 9 shows the fully ice formed upper surface of airfoil and the dynamic pressure changes are severe around the ice formed region. The dynamic pressure increased enormously from 31.2kPa to 38.1kPa due to the complete ice accretion. It affects the critical Mach number around the airfoil and turbulent flow separation behavior in the unstalled region [16]. Hence, the resulting C_p distribution profile decreases the local Mach number through CD rise thus affecting the stability of the airplane yet the AoA is 0°. The dynamic pressure at leading edge is around 7.8kPa due to the ice formation and the maximum dynamic pressure of 38.1kPa occurs at the top surface of the airfoil.

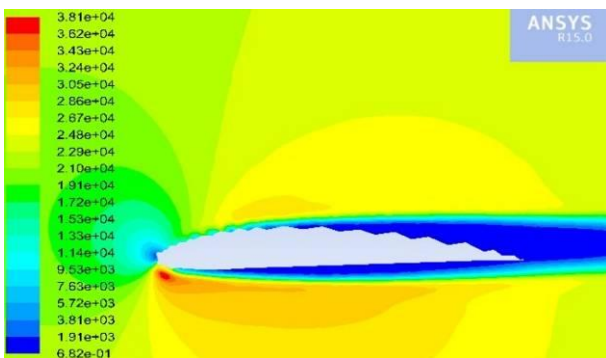


Fig. 9: Dynamic pressure with full ice on top (At 0° AoA)

Fig. 10 highlights the dynamic pressure profile at 3 deg AoA with fully iced condition at top surface of the airfoil. This profile shows the fully iced airfoil with slightly increased AoA and the dynamic pressure change is noted and the profile change around the airfoil is visualized. The dynamic pressure was decreased to 34.4 kPa from 36.8 kPa. The gradual reduction in dynamic pressure profile shows that the aerodynamic properties are affected around the wing instantaneously. It reveals a fact that the need of Anti-icing requirements increases in proportion to the Aspect Ratio (AR). The dynamic pressure at leading edge is around 8.6 kPa due to the ice formation and the maximum dynamic pressure of 34.4 kPa occurs at the upper surface of the airfoil. Fig. 11 shows the dynamic pressure profile at 6° AoA with fully iced condition at the upper surface of airfoil. This profile is obtained for fully iced condition with 6° AoA and it is realized that the dynamic pressure immensely decreased from 36.2kPa to 29.9kPa as compared with no ice conditions. This enormous drop in dynamic pressure and comparison of all the equivalent velocity profiles clearly states that the ice accretion decreases the dynamic pressure which indirectly affects all the other aerodynamic factors and the stability of the airplane. The dynamic pressure at leading edge is around 4.48kPa because of the ice accretion and the maximum dynamic pressure of 29.9kPa occurs at the top surface of the airfoil. The instantaneous Mach number changes due to rime ice accretion are difficult to predict and it affects the control components significantly. The ice accretion may also leads to any fatal accidents in the event of

insufficient anti-icing or de-icing issues. Hence, the icing problem should be analyzed and necessary alternate methods have to be prepared to ensure the completely safe air transport in the near future.

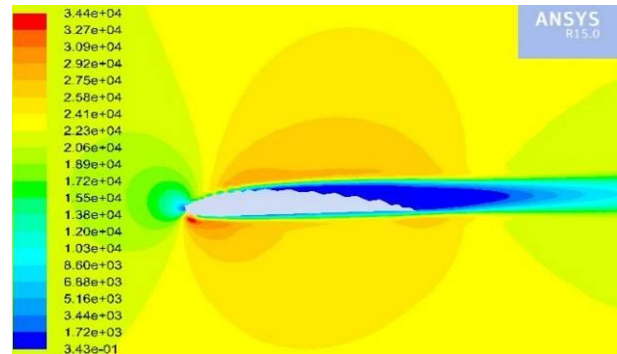


Fig. 10: Dynamic pr. with full ice on top (At 3° AoA)

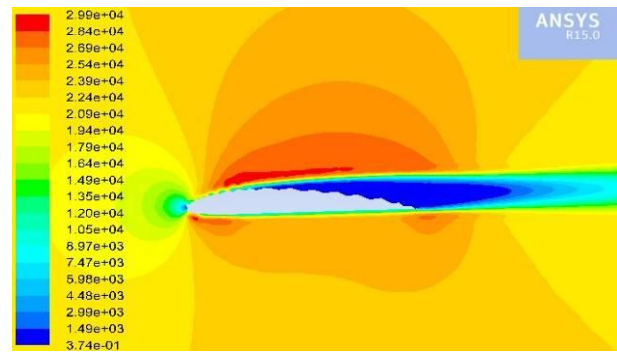


Fig. 11: Dynamic pressure with full ice on top (At 6° AoA)

2.4. Graph for mach number comparison:

Fig. 12 presents the variation of the Mach number obtained against the number of ice bubbles accretion over time. From the numerical investigation, it is concluded that the Mach number decreases as the ice accumulation increases in accordance with the AoA. However, the operating altitude and equilibrium CL are the other two factors that determines the severity of Mach number changes against ice accretion.

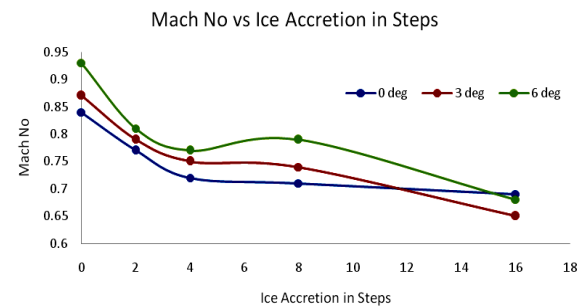


Fig. 12: Ice bubble accretion vs Mach number distribution at various AoA

3. Conclusions

Airplanes should fly at high altitudes and the icing problem is encountered at every hour of flight. Present anti-icing systems are efficient to avoid the ice accretion problems by compromising a certain percentage of fuel costs. Hence, the purpose of the present numerical investigation is to propose novel preventative measures to overcome the icing problem in airplanes through flow

control strategies. The methods to be used should be cost effective and efficient. Hence, the change in aerodynamic forces is studied through the numerical analysis. It shows that the constant increase in velocity distribution around the airfoil because of the ice formation. Since the icing problem cannot be completely avoided the effects has to be minimized as low as possible. The velocity increment observed is mainly due to the fat airfoil that leads to large drag rise. If the surface is superhydrophobic then this drag force would assist for the removal of ice layers without any other anti-icing systems.

Hence on the ground of detailed literature studies, it is found that superhydrophobic coating will be an effective measure for the icing problems in airplane surfaces. Since superhydrophobic coating are anti-icing agent it prevents from the formation of ice rather than clearing the ice after it is formed on the aircraft surfaces. The superhydrophobic coatings are practically used in the region of cold countries to prevent ice on power transmission cables and it was found to be yielding good results, hence superhydrophobic coatings will be a best solution for the icing problems in aircraft.

REFERENCES:

- [1] A. Heinrich, R. Ross, G. Zumwalt and J. Provorse. 1991. *Aircraft Icing Handbook: FAA.*, Atlantic city.
- [2] D.N. Anderson and A.D. Reich. 1997. Tests of the performance of coatings for low ice adhesion, *Proc. NASA Tech. Mem. 107399, AIAA 35th Aerospace Sciences Meeting*, Cleveland, Ohio. <http://dx.doi.org/10.2514/6.1997-303>.
- [3] S. Kimura, Y. Yamagishi, A. Sakabe, T. Adachi and M. Shimanuki. 2007. A new surface coating for prevention of icing on airfoils, *Proc. SAE Aircraft and Engine Icing Int. Conf.*, Seville, Spain. <http://dx.doi.org/10.4271/2007-01-3315>.
- [4] C. Ryerson. 2009. Icing and offshore arctic oil operations safety, *Proc. 13th IWAIS*, Andermatt, Switzerland.
- [5] N. Dalili, A. Edrisy and R. Carriveau. 2009. A review of surface engg. issues critical to wind turbine performance, *Renewable and Sustainable Energy Reviews*, 13(2), 428-438. <http://dx.doi.org/10.1016/j.rser.2007.11.009>.
- [6] C. Antonini, F.J. Carmona, E. Pierce, M. Marengo and A. Amirfazli. 2009. General methodology for evaluating the adhesion force of drops and bubbles on solid surfaces, *Langmuir*, 25(11), 6143-6154. <http://dx.doi.org/10.1021/la804099z>.
- [7] Y. Boluk. 1996. *Adhesion of Freezing Precipitates to Aircraft Surfaces*, Transport Canada Publication, TP 12860E, Canada.
- [8] C. Antonini, A. Amirfazli and M. Marengo. 2010. Statistical analysis of water drop impact on surfaces with variable wettability, *Proc. 23rd Annual Conf. Liquid Atomization and Spray Systems*, Brno, Czech Republic.
- [9] L. Cao, A.K. Jones, V.K. Sikka, J. Wu and D. Gao. 2009. Anti-icing super hydrophobic coatings, *Langmuir*, 25(21), 12444-12448. <http://dx.doi.org/10.1021/la902882b>.
- [10] H.A. Porte and T.E. Nappier. 1963. *Coating Material for Prevention of Ice and Snow Accumulations*, U.S. Naval Civil Eng. Lab., TN 541, Port Hueneme, CA.
- [11] R.N. Wenzel. 1936. Resistance of solid surfaces to wetting by water, *Industrial and Engg. Chemistry*, 28, 988-994. <http://dx.doi.org/10.1021/ie50320a024>.
- [12] D. Richard, C. Clanet and D. Quere. 2002. Contact time of a bouncing drop, *Nature* 417, 811. <http://dx.doi.org/10.1038/417811a>.
- [13] A.B.D. Cassie and S. Baxter. 1944. Wettability of porous surfaces, *Trans. Faraday Society*, 40, 546-551, Guelph. <http://dx.doi.org/10.1039/tf9444000546>.
- [14] M. Papadakis, H.W. Yeong, S.C. Wong and S.H. Wong. 2010. Comparison of experimental and computational ice shapes for an engine inlet, *AIAA 2010-7671*, Canada.
- [15] C. Antonini, M. Innocenti, T. Horn, M. Marengo and A. Amirfazli. 2011. Understanding the effect of superhydrophobic coatings on energy reduction in anti-icing systems, *Cold Regions Science and Technology*, 67, 58-67. <http://dx.doi.org/10.1016/j.coldregions.2011.02.006>.
- [16] J.B.R. Rose and G.R. Jinu. 2015. Influence of aeroelastic control reversal problem in the airplane lateral stability modes, *Proc. IMechE Part G: J. Aero. Engg.*, 229(3), 517-533. <http://dx.doi.org/10.1177/0954410014537241>.